



Malaria in Burkina Faso (West Africa) during the twenty-first century

Yves M. Tourre  · Cécile Vignolles · Christian Viel · Fazlay S. Faruque · John B. Malone

Received: 17 March 2017 / Accepted: 20 March 2019
© Springer Nature Switzerland AG 2019

Abstract Temperature and rainfall predicted for the twenty-first century by global coupled models as reported by IPCC, (2014a, and b) were obtained regionally for Burkina Faso and through the Paluclim project, 2011–2014. One of the goals of this project was to assess the upcoming evolution of malaria transmission dynamics. From an impact model on malaria risk linked to climate variability, temperature and rainfall indices were derived. Malaria transmission dynamics were then predicted using the derived temperature and rainfall for the twenty-first century. Similar to the historical evidence of rainfall being an important factor for regulating the seasonal density of malaria vectors, this study also

reports a definitive link between low-frequency rainfall variability and malaria in the region under the influence of the Atlantic Multidecadal Oscillation (AMO). This finding can be used by local stakeholders involved with the geography-based population health planning. Moreover, the predicted increase in temperature during the twenty-first century suggests a reduction of larvae survival in Burkina Faso and thus the malaria risk. More generally, the temperature increase could become a new limiting factor for malaria transmission dynamics in the Sahel Region (as reported by Mordecai et al. (2013).

Keywords Malaria · Atlantic multidecadal oscillation · Sahel · Climate change

This article is part of the Topical Collection on *Geospatial Technology in Environmental Health Applications*

Y. M. Tourre (✉)
LDEO of Columbia University, Palisades, NY, USA
e-mail: yvestourre@aol.com

C. Vignolles
CNES, Toulouse, France
e-mail: cecile.vignolles@cnes.fr

C. Viel
Météo-France, Toulouse, France
e-mail: christian.viel@meteo.fr

F. S. Faruque
University of Mississippi Medical Center, Jackson, MS, USA
e-mail: ffaruque@umc.edu

J. B. Malone
Louisiana State University, Baton Rouge, LA, USA
e-mail: vtmalon@lsu.edu

Introduction

Malaria is responsible for 61% of hospitalizations and 30% of deaths yearly in Burkina Faso, which belongs to the Sahel Region in West Africa. Mortality, primarily among children under 5 years old, has been steadily increasing by more than 4% every year. Interestingly, Paaijmans et al. (2012) and more recently Asare et al. (2016) reported that warmer pond water temperature should reduce the vectorial capacity of malaria mosquitoes and thereby should reduce the burden due to malaria.

The Paluclim project investigated the impacts of climate variability and climate change in Burkina Faso (Fig. 1) for the twenty-first century (Vignolles et al. 2016). This project employed the tele-epidemiology approach (a term coined by Marechal et al. 2008), which

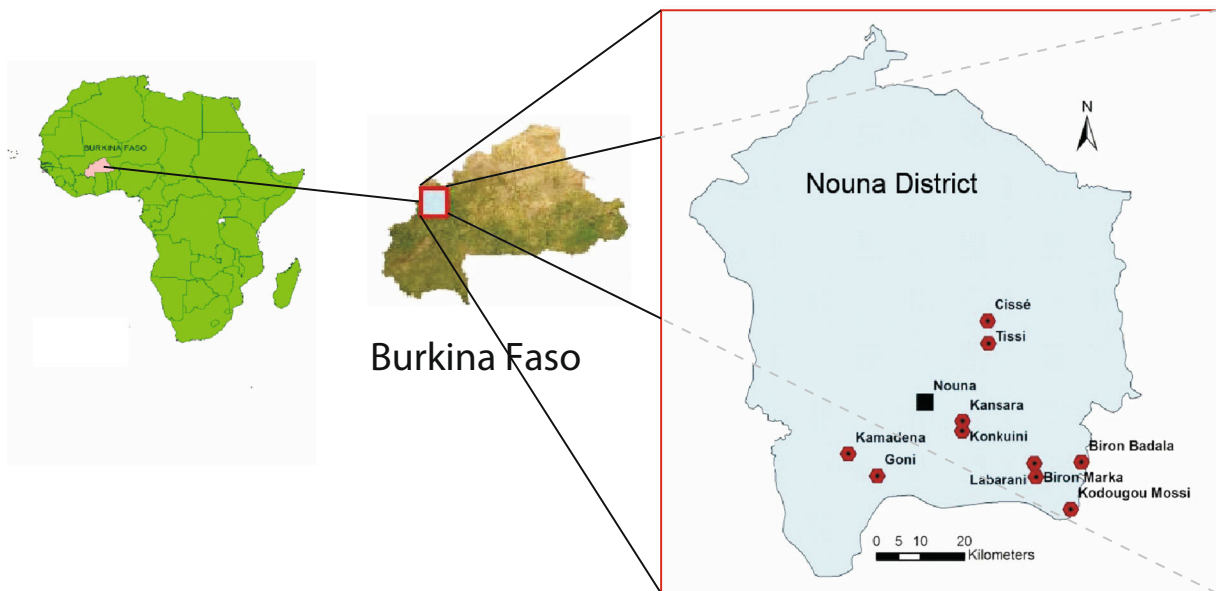


Fig. 1 Localization of the Nouna Region in Burkina Faso (4.1/3.5° W and 12.4/13° N) in West Africa (left). The red hexagons are the 10 villages where meteorological (i.e., from rain gages and

min-max thermometers) and entomological data was obtained. This region belongs to the Sahel (i.e., 800 mm of rainfall during the rainy season from June to September)

required comprehensively combining environmental and climatological conditions and involving entomologists to predict the impacts on infectious diseases, including malaria. Data from the space (CNES 2008) were also used to portray the big picture of the study area. Indeed, tele-epidemiology is designed to analyze the relations between climate, environment, and health and to highlight links between the emergence and spread of infectious diseases with geospatial data from Earth Observation Systems satellites (Walz et al. 2015; UNOOSA 2018).

The tele-epidemiology approach, used in the Paluclim project, was then applied in this study to predict malaria in the rural Nouna Region of northern Burkina Faso. The objective of the present research was to study the details of the effects of low-frequency climate variability and change on malaria risk, with a specific focus on spatio-temporal variability associated with the Atlantic Multidecadal Oscillation (AMO) and climate change issues.

The suitable conditions for malaria transmission, ~ 71% by *Plasmodium falciparum* (Gneme et al. 2013), were derived by studying the relationship between temperature, sporogony, vector survival, and length of the larval cycle (Dambach et al. 2012).

Moreover, it has been shown that an important parameter for malaria risk in Burkina Faso is the monthly

total rainfall with an 80-mm threshold for the first month of a given 3-month sequence of time during the rainy season (Tourre et al. 2017). Finally, the knowledge of the AMO phases and its low-frequency variability (1856 to present, obtained from NOAA) may be very important for adaptation procedures by regional health information systems (HIS) involved in climate change-related health planning. The AMO changed phases in the mid-1990s (i.e., from negative to positive values) and was associated with rainfall increases over the Sahel (see also Zhang and Delworth 2006; Paz et al. 2008). According to the climate projections for the twenty-first century, and preliminary results from models also used for the CORDEX experiment (2013, courtesy of Dr. Samuel Somot from CNRM), environmental conditions are going to change over West Africa (Roudier et al. 2011) particularly temperature.

In this study, a pronounced tendency for a decreased development of malaria in the Nouna region is identified along with the increase of the maximum mean yearly temperature from numerical models during the twenty-first century. As such and based upon output from the Coupled Model Inter-comparison Project Phase 5 or CMIP-5 (see details in the next section), different radiative scenarios for temperature and rainfall variability are compared to that during the 1983–2011 period.

Data and methods

To understand the effects of climatic conditions on malaria risk, an impact model based on several prior studies (Craig et al. 1999; Emmert et al. 2011), modified for the MARA project (Tanser et al. 2003), is used here. Climate indices (IND) favoring local malaria diffusion are computed with values going from 0 (or U for unsuitable) to 1 (or S for suitable). As reported in Craig et al. (1999), the sigmoidal fuzzy function from IDRISI (2018) was used to convert climate data between unsuitable (U) and suitable (S) conditions. The ranges for the rainfall and temperature indices are then computed for suitable conditions (see Table 1 in Tourre et al. 2017) and are from 0 to 10. The normalized means are between 2 and 4 for precipitation and 6 and 8 for temperature as shown in Fig. 2.

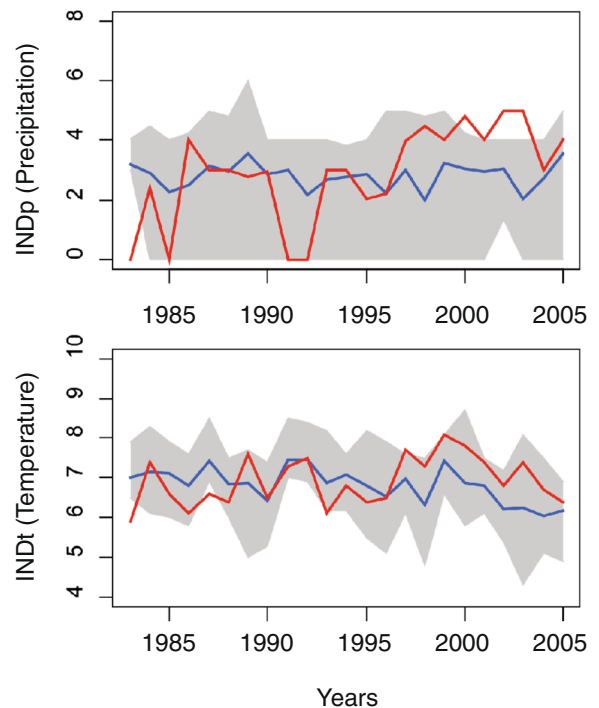
Historical data was then observed, while simulated/predicted data from different models (see below) were adjusted from the quantile-quantile method during the 1983–2005 period. Finally, the adjusted values from in situ data were converted into indices for rainfall (INDp) and temperature (INDt) for malaria risk.

The prediction and climate scenarios for the twenty-first century were subsequently obtained through the

global simulations from the Coupled Model Inter-comparison Project Phase 5 or CMIP-5 (Taylor et al. 2012). More than 300 projections or Representative Concentration Pathways (RCP) have been analyzed. For the Paluclim project scenarios, RCP45 and RCP85 were chosen, where RCP45 represents a radiative forcing of 4.5 W/m^2 (or watts per unit area) in 2100, equivalent to 660 CO_2e (or the concentration of CO_2 that would cause the same level of radiative forcing, in parts per million by volume, ppmv) and leading to a plateau at the end of the period. The RCP85 scenario represents a radiative forcing larger than 8.5 W/m^2 on and after 2100, equivalent to 1370 CO_2e with a continuous increase. The latter scenario is seen as the most pessimistic and extreme scenario (i.e., with very little regulations on greenhouse gas emissions).

For rainfall output, a total of eight models was used, six of them models were used for Tmin and Tmax temperatures; all models were obtained from the Institute Pierre Simon Laplace (IPSL-CM5A5 LR and MR). Some models have been implemented by the Canadian Centre for Climate Modeling and Analysis (CCma-CanESM2), the Centre National de Recherches Météorologiques (CNRM-CM5), Hadgem2-ES, INM-CM4, Atmosphere and Ocean Research Institute (The

Fig. 2 Precipitation index INDp (top) and temperature index INDt (bottom) during the 1983–2005 period, after quantile-quantile adjustment for the simulated data. In red are the observations in the Nouna Region, and in blue are the mean simulated values. In gray are the spread or uncertainties from the models around the mean. After 1996, the INDp values are not only larger than observed values but are also getting out of the statistical range (2000 until 2004)



University of Tokyo), and MIROC5 (Model for Interdisciplinary Research on Climate). The grid-point systems for all models were 2.5° . The multi-model (or ensemble) approach was used, to assess environmental climate conditions associated with malaria risk. Four grid points were taken around Nouna, from which time series of average rainfall, and minimum and maximum temperatures were extracted. Since only one simulation was used per model, the uncertainties could not be included in the results. Nevertheless, the multi-model approach allows assessment of environmental conditions associated with malaria risk during the twenty-first century (Knutti et al. 2010).

Results and discussion

The capacity for models to reproduce (after the quantile-quantile adjustment) the indices values for favorable malaria conditions, and from rainfall and temperature indices are shown in Fig. 2. The multi-model ensemble displays a large variation for rainfall INDp index (Fig. 2, top). The blue curve is the mean for historical simulation, and the red curve is the mean from observations (i.e., it is the precipitation index for favorable conditions for malaria development during 1983–2005). Despite the large dispersion (shaded area, representing the model uncertainties), the index is outside the possible values particularly during the positive phase of the AMO, post-1996. This strongly suggests a possible underestimation of rainfall amount by the models. The latter must modify the values of the index. Nevertheless, this is not the case for the INDt index (Fig. 2, bottom), where simulated and observed values are much more coherent, i.e., with a much smaller spread.

The lack of the AMO climate signal is obvious when the probability density function of the INDp (according to the observed and simulated AMO phases) is displayed for historical values during 1983–2005 (Fig. 3, top). The observed AMO anomalies for the 1983–2005 period are negative from 1983 to 1996 and positive from 1996 to 2005.

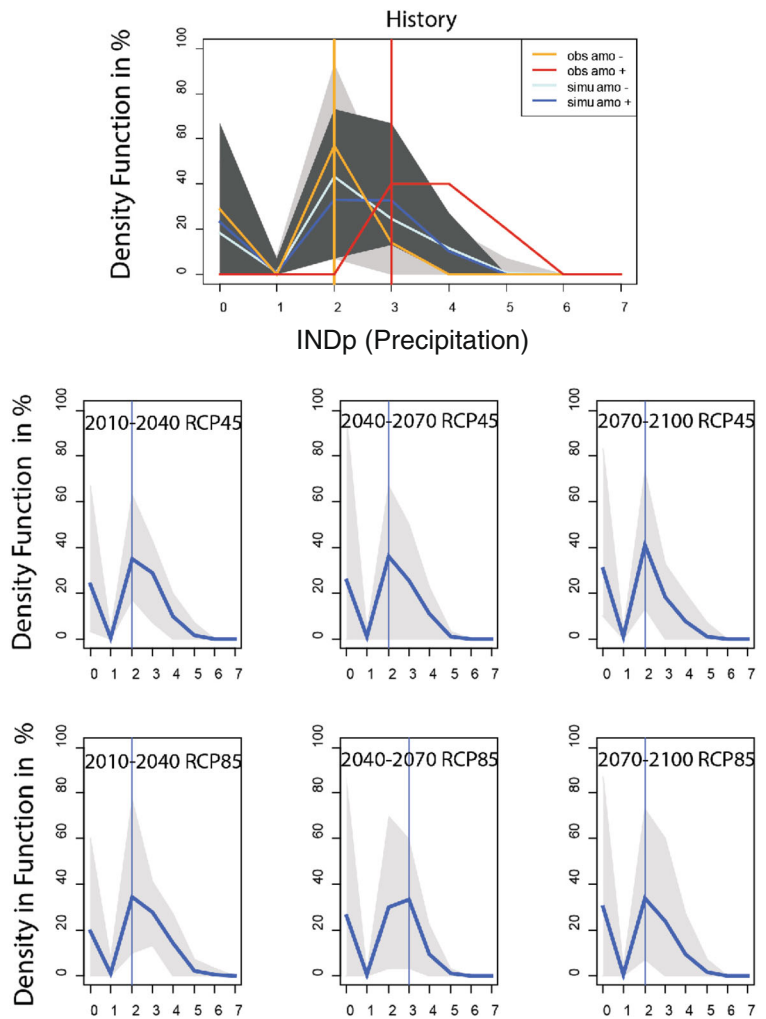
Dark (light) blue curves are for mean simulations when the AMO is positive (negative). The dark/light gray shaded zones are for the spread from the mean during positive (negative) phase of the AMO. In the middle and during the negative phase of the simulated AMO, the density peak is clearly established for an index value of 2 (light blue curve). On the contrary

during a simulated positive AMO (dark blue curve), the density curve displays a plateau with index values of 2–3. For the observed values (red curve), the index values are between 3 and 4. It can be seen that there is a lag between simulated and observed values. In general, the favored hypothesis from the probability density functions is that the simulated rainy seasons are shorter during the positive phase of AMO. Nevertheless, the total amount of observed rainfall during the latter on interannual time scales could be increased (Paz et al. 2008). Since the AMO is a multi-decadal climate signal, variability of the mean, averaged over 30-year periods, was computed for the 2010–2100 period using the RCP 45 and RCP85 scenarios. The mean for the density functions along with their spread (gray shading) is displayed in Fig. 3 (RCP45 middle, and RCP85 bottom).

Except for the 2040–2070 period and for the RCP85 scenario, the distribution is somewhat equivalent to the one obtained during the AMO negative phase (historical data). In general, the rainfall conditions are not favorable, but the spread around the means is quite large. Under the RCP85 scenario, the 2040–2070 (Fig. 3, bottom, middle), the probability density function distribution resembles somewhat to that of historical distribution during AMO-positive phases with an index peak at 3.

In Fig. 4, the same information as for Fig. 3 is shown but for INDt. At the top of Fig. 4, the historical values of the index are shown also as a function of AMO phases, whilst at the bottom, the density functions are displayed every 30 years starting in 2010 (middle for the RCP45 scenario, bottom for the RCP 85 scenario). Only the red curve (Fig. 4, top) displays a maximum value of 7 for the density function during the AMO-positive phase. For the other curves in Fig. 4 (top), most of the peaks for the density functions are for a temperature index of 6. For a 30-year period starting in 2010 (Fig. 4, bottom left) and for the two scenarios RCP45 (middle) and RCP85 (bottom), the conditions are already less favorable than during the historical period with a peak of 5 for the index. On average, the RCP45 does not show major changes before 2070, the time during which the temperature conditions should start to make it difficult for the survival of larvae and adult mosquitoes and thus of malaria diffusion. On the contrary, the RCP85 scenario displays changes as soon as 2040 with a very low peak value of 3 for the index. The 2070–2100 period displays an extremely low peak value of 1 for the index. Thus,

Fig. 3 (Top) Probability density function for IND_p values (abscissa) during the 1983–2005 period, considering the influence of AMO phases. In red (orange) are observations during years when the AMO is positive (negative). Dark (light) blue curves are for mean simulations when the AMO is positive (negative). The dark/light gray shaded zones are for the spread from the mean during positive (negative) phase of the AMO. (middle) The density distribution of the index is displayed for RCP45 every 30 years starting in 2010. (Bottom) The density distribution of the index is displayed for the RCP85 scenario also starting in 2010. The blue curve is for the mean, and the gray shading represents the spread (uncertainties) around the mean. Peak values of the index are identified by a line for each 30-year period. Values for the index are on the abscissa



whatever the rainfall conditions between 2070 and 2100 might be, the suitability of environmental conditions could be strongly diminished for malaria transmission.

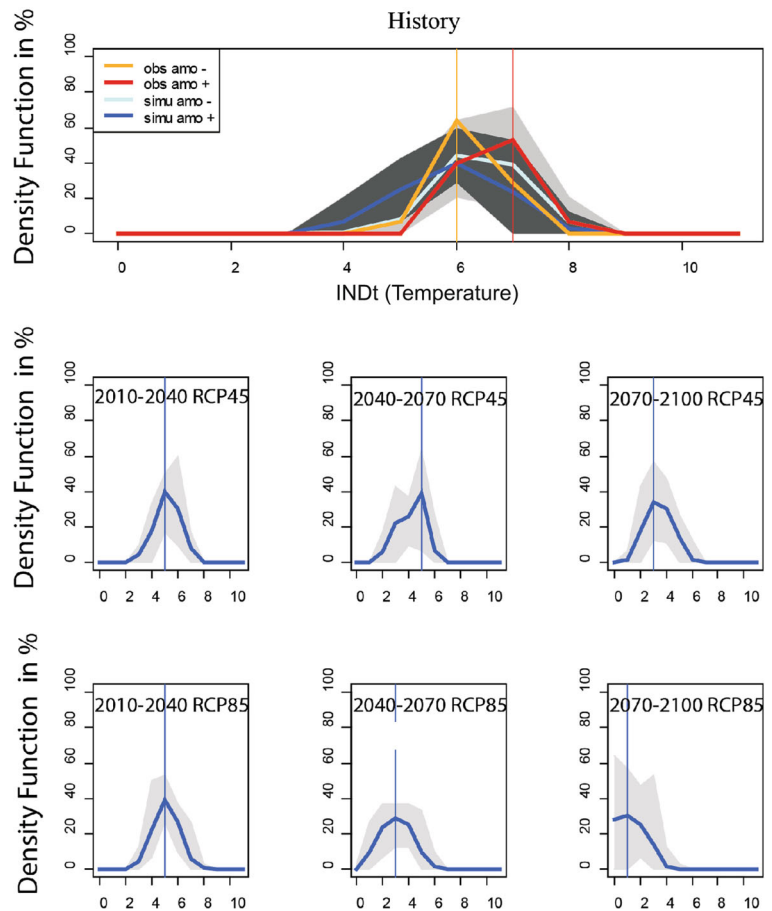
Large interannual variability is evident for IND_p (Fig. 5, left) with a small tendency leading to unfavorable conditions when compared to the historical period. Before 2040, the RCP85 scenario seems more favorable than the RCP45 scenario. However, due to the large spread of IND_p, no significant conclusions for malaria risk can be drawn. On the contrary, the tendency of the IND_t (Fig. 5, right) indicates less and less favorable conditions for malaria in the Nouna Region, for both RCP45 and RCP85 scenarios. This large tendency is associated with the evolution of the annual maximum temperature.

Finally, the temperature evolution itself is displayed in Fig. 6 for the period 1980–2100, with the dashed

orange line at the bottom representing the temperature mean for the so-called historical period (1983–2005), while the dashed red line is the limit for the temperature at which the conditions will become extremely unfavorable (2090). The RCP45 scenario in light blue is for an increase of the mean temperature in Nouna of 3 °C, while the RCP85 scenario in dark blue is for more than 5 °C. The temperature thus attained of 40 °C (RCP85) at the end of the twenty-first century explains the rapidly decreasing values of the IND_t index in Fig. 5.

No visual signs for malaria risk increase are linked to rainfall. Indeed, the foreseen rainfall distribution is somewhat similar to that during the 1983–2005 period. Thus, over the Nouna Region, the climate tendency, without the natural variability (including that of the AMO), does not change significantly the rainfall index for changes in malaria risk (Figs. 2 and 3).

Fig. 4 Same as in Fig. 3 except for the probability density function of the temperature index or INDt



The malaria risk evolution is assessed using slices of 30-year period for both scenarios. The temperature evolution during the 2010–2040 displays conditions already less favorable than during the historical period. The peak for the density function is indeed attained for an index of 5 (and for both scenarios). For mean values, the RCP45 scenario does not reflect major changes before the 2070–2100 period, when temperature is already highly limiting the malaria risks. On the contrary, the RCP85 scenario leads to major changes as soon as the middle of the twenty-first century with a peak of 3. During the 2070–2100 period, temperature conditions are associated with a very low index of 1 (Fig. 5).

Conclusions

The AMO and its linkages with rainfall variability are important for malaria evolution. It has been found that during the 1983–2012 period, monsoon seasons

were shorter from 1983 to 1996 and then lasted longer after 1996 when the AMO was positive (Tourre et al. 2017) favoring malaria development.

Whilst climate change could modify the AMO variability, it could also, through temperature increase, modify the evolution of several human infectious diseases, including malaria, cholera, and dengue. In Burkina Faso, for example, after a continuous increase of malaria transmission up to 60 cases per 1000 humans in 2001, it has held steady since then at 40 cases per 1000 in humans (WHO 2003, 2008). Although it is known that a major effort has been made to introduce widespread use of impregnated bed nets during this time, the complexities of the epidemiology of malaria present difficult challenges for establishing a distinction between climatic and non-climatic causal effects (Ostfeld et al. 2008).

Based on the output of the models, large mean monthly temperature increases in the Nouna Region are predicted to lead to malaria risk reduction;

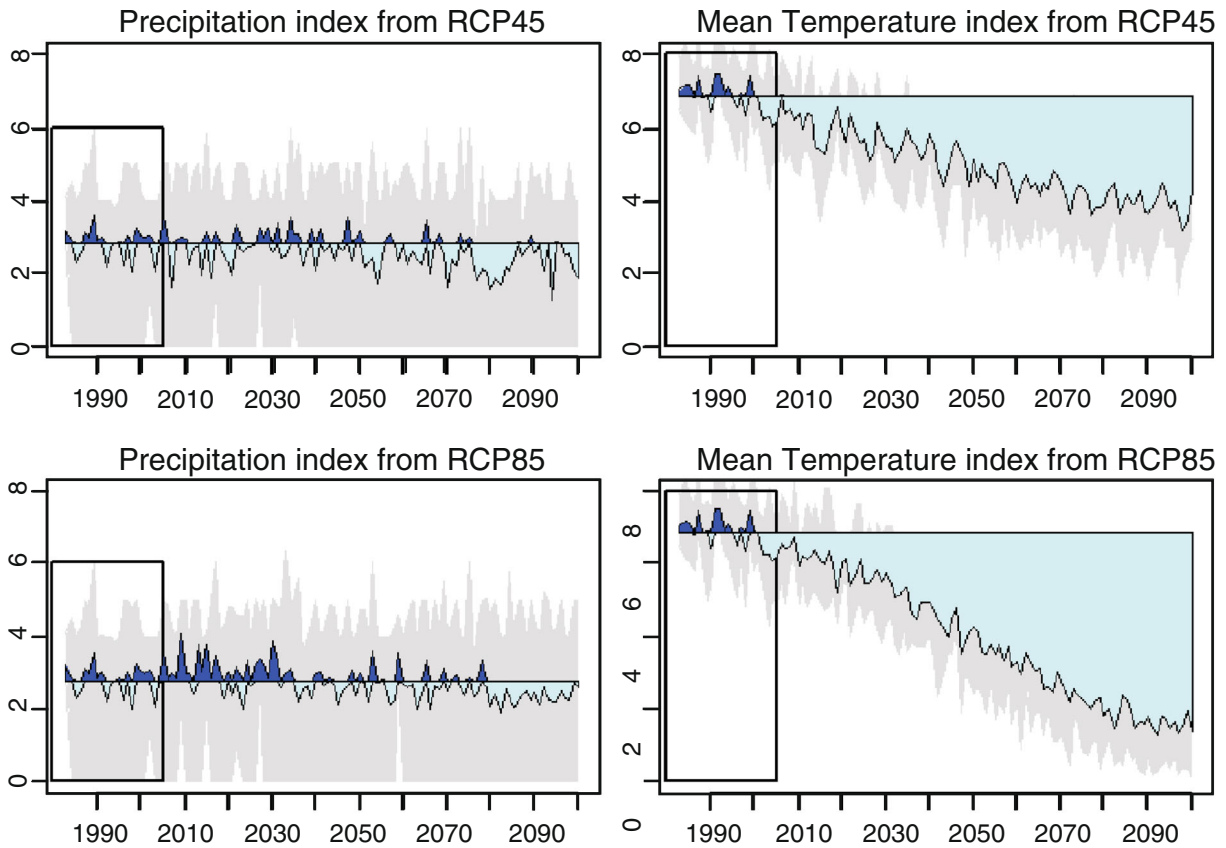


Fig. 5 Mean evolution (with spread) of the yearly index values for favorable conditions of the rainfall index INDp (left) and the temperature index INDt (right) for the 1983–2100 period. Values of the indices are on the ordinates. Post-2005 (highlighted by the black rectangle), the evolutions are for the climate scenarios

RCP45 (top) and RCP85 (bottom). The dark blue (light blue) shaded areas are for values above (below) the means computed for the 1983–2005 historical period. Within the black rectangle results until 2005 are very similar for both scenarios (RCP45 and RCP85)

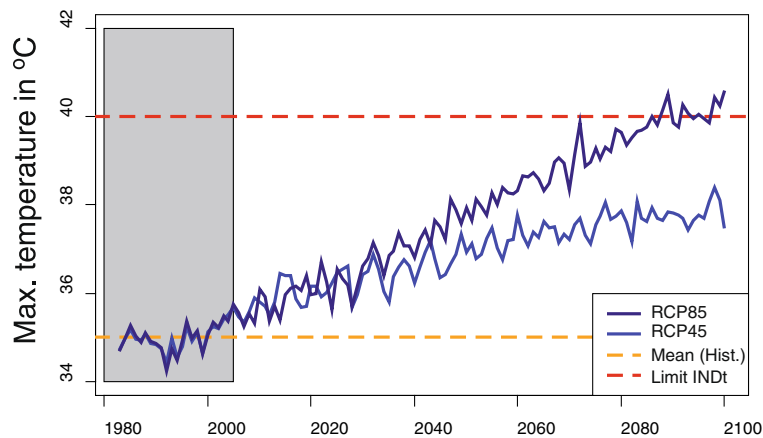


Fig. 6 Evolution of mean maximum temperature from the multi-model’s ensemble with two different RCP scenarios as described in the text. Once again until 2005, evolutions are similar (within gray-shaded rectangle) and then spread rapidly after 2030 when

RCP45 (light blue) and RCP85 (dark blue) scenarios are compared. The red dashed line is for the upper limit of T_x for malaria diffusion, which is attained near the end of the twenty-first century (around 2085) by using the RCP85 scenario

temperature thus becomes a limiting factor for malaria risks in the face of predicted climate change in the Nouna region of Burkina Faso. For example, the dominant *A. gambiae*, which was sampled during this study does not adapt well to hotter conditions (Kirby and Lindsay 2004). This is a very important change to consider since malaria has always been of great public health concern. It seems likely that "... malaria will be a vector-borne disease that is both sensitive to long-term climate change reductions, and that it will also vary seasonally in highly endemic areas" (Patz et al. 2003).

In this paper, the results suggest the potential for malaria (and other infectious diseases of Africa) to invade southern Europe where conditions may become more suitable owing to lower maximum temperatures than in the Sahel for the vector mosquitoes' ecological and meteorological niches. For example, an assessment in Portugal projected an increase in the number of days per year suitable for malaria transmission (Casimiro et al. 2006). Thus, climatic change factors may favor transmission, increased vector density, and re-emergence of malaria in Europe (Rogers and Randolph 2000). It is recognized that socio-economic factors, building codes, land use, and treatment could also slow down the likelihood of climate-related epidemics. In any case whilst the rainfall amount and threshold certainly determine mosquito abundance, temperature will have its major effect on development of the malaria parasites in the vector. Malaria risk may thus be considerably reduced at the end of the twenty-first century in the Sahel as compared to current risk. Faruque et al. (2014) have developed a web-based real-time syndromic surveillance system, known as GeoMedStat, with disease and environmental condition mapping capabilities that may be of value to epidemiologists and public health officials for interpretation and analysis of both routine and new outbreak-related health data that can potentially be linked to climate change impacts (Taylor et al. 2016). The Healthy Futures project in East Africa adopted basically the same approach for framing infectious disease risks (Oppenheimer et al. 2014) and becomes a key vehicle for communicating main results through its Healthy Futures atlas. The latter obtained input from stakeholders, including health decision makers in east African countries like Burundi, Kenya, Rwanda, Tanzania, and Uganda. In the climate change context, the same activity could be developed in the Sahel over West Africa.

Acknowledgements The authors would like to thank CNES for managing and Dr. Vanessa Machault and Dr. Flore Mounier for participating among others in the Paluclim project. Thanks to Dr. Philippe Dandin and Phippe Bougeaut, former directors of Météo-France Climatology and CNRM divisions of Météo-France. Thanks to Ronnydeux for formatting the final figures. Thanks also to our mentor Dr. Jean-Pierre Lacaux. Dr. Tourre would like to thank Dr. Sean C. Solomon, the new director of Lamont-Doherty Earth Observatory (LDEO), for supporting his research. This is LDEO contribution no. 8270.

References

- Asare, E. O., Tompkins, A. M., Amekudzi, L. K., & et al., (2016). Mosquito breeding site water temperature observations and simulation towards improved vector borne diseases models for Africa. *Geo. Health*, 11, Healthy Features.
- Casimiro, E., Calheiros, J., Santos, F. D., & Kovats, S. (2006). National of human health effects of climate change in Portugal: approach and key findings. *Environmental Health Perspectives*, 114(12), 1950–1956.
- CNES. (2008). Method for tele-epidemiology. Patent pending # PCT/FR2009/050735.
- CORDEX. (2013). [http://cordex2013.wcrp-climate.org/Region 5](http://cordex2013.wcrp-climate.org/Region%205), Craig, M. H., Snow, R. W., & le Sueur, D. (1999). A climate-based distribution model of malaria transmission in sub-Saharan Africa. *Parasitology Today*, 15(3), 105–111.
- Dambach, P., Machault, V., Lacaux, J.-P., Vignolles, C., Sie, A., & Sauerborn, R. (2012). Utilization of combined remote sensing techniques to detect environment variables influencing malaria vector densities in rural West Africa. *International Journal of Health Geographics*, 11, 8.
- Emmert, V., Finks, A. H., Jones, A. E., & Morse, A. P. (2011). Development of a new version of the Liverpool Malaria Model. Refining the parameters settings and mathematical formulation of basic processes based on a literature review. *Malaria Journal*, 10, 35.
- Faruque, F. S., Li, H., Williams, W. B., Waller, L. A., Brackin, B. T., Zhang, L., Grimes, K. A., & Finley, R. W. (2014). GeoMedStat: an integrated spatial surveillance system to track air pollution and associated healthcare events. *Geospatial Health*, 8(3), S631–S646.
- Gneme, A., Guelbeogo, W. M., Riehle, M., Diarra, A., Kabre, G. B., Sagnon, N., & Vernick, K. D. (2013). *Plasmodium* species occurrence, temporal distribution and interaction in a child-aged population in rural Burkina Faso. *Malaria Journal*, 12(1), 67.
- IDRISI. (2018). <https://clarklabs.org/terset/idrisi-gis/> Clark Labs, Clark University 950 Main St., Worcester MA 01610 USA. Accessed January 2019
- IPCC. (2014a). Fifth assessment report. <http://www.ipcc.ch/report/ar5/wg2/>. Accessed March 2019
- IPCC. (2014b) Climate change 2014: Impacts, adaptation, and vulnerability. Part B: Regional aspects. Contribution of working group II to the fifth assessment report of the intergovernmental panel on climate change [Barros, V.R., C.B. Field, D.J. Dokken, M.D. Mastrandrea, K.J. Mach, T.E. Bilir, M.

- Chatterjee, K.L. Ebi, Y.O. Estrada, R.C. Genova, B. Girma, E.S. Kissel, A.N. Levy, S. MacCracken, P.R. Mastrandrea, and L.L. White (eds.]. Cambridge University Press, Cambridge, United Kingdom and New York pp. 688.
- Kirby, M. J., & Lindsay, S. W. (2004). Responses of adult mosquitoes of two sibling species, *Anopheles arabiensis* and *A. gambiae* s.s. (Diptera: Culicidae) to high temperatures. *Bulletin of Entomological Research*, 94(5), 441–448.
- Knutti, R., Abramowitz, G., Collins, M., Eyring, V., Gleckler, P. J., Hewitson, B., & Means, L. O. (2010). Good practice guidance paper on assessing and combining multi model climate projections, IPCC working group I technical support unit. In: Meeting report of the intergovernmental panel on climate change expert meeting on assessing and combining multi model climate projections. University of Bern, Bern.
- Marechal, F., Ribeiro, N., Lafaye, M., & Guell, A. (2008). Satellite imaging and vector-borne diseases: the approach of the French National Space Agency (CNES). *Geospatial Health*, 3(1), 1–5.
- Mordecai, E. A., Paaijmans, K. P., Johnson, L. R., Balzer, C., Horin, T. B., de Moor, E., McNally, A., Pawar, S., Ryan, S. J., Smith, T. C., & Laffery, K. D. (2013). Optimal temperature for malaria transmission is dramatically lower than previously predicted. *Ecology Letters*, 16(1), 22–30.
- NOAA, AMO time-series (1856-present). https://www.esrl.noaa.gov/psd/gcos_wgsp/Timeseries/AMO/. Accessed March 2019
- Oppenheimer, M., Campos, M., Warren, R., Birkmann, J., Luber, G., O'Neill, B., & Takahashi, K. (2014). Emergent risks and key vulnerabilities. In C. B. Field, V. R. Barros, D. J. Dokken, K. J. Mach, M. D. Mastrandrea, T. E. Bilir, M. Chatterjee, K. L. Ebi, Y. O. Estrada, R. C. Genova, B. Girma, E. S. Kissel, A. N. Levy, S. MacCracken, P. R. Mastrandrea, & L. L. White (Eds.), *Climate change 2014: impacts, adaptation, and vulnerability. Part A: global and sectoral aspects. Contribution of Working Group II to the Fifth Assessment Report of the Intergovernmental Panel on Climate Change* (pp. 1039–1099). Cambridge: Cambridge University Press.
- Ostfeld, R. S., Keesing, F., & Eviner, V. T. (Eds.). (2008). *Infectious disease ecology: effects of ecosystems on disease and of disease on ecosystems*. Princeton: Princeton University Press.
- Paaijmans, K. P., Blandford, S., Chan, B. H. K., & Thomas, M. B. (2012). Warmer temperature reduce the vectorial capacity of malaria mosquitoes. *Biology Letters*, 8, 465–468.
- Patz, J. A., Githeko, A. K., McCarty, J. P., Hussein, S., Confalonieri, U., & De Wet, N. (2003). Climate change and infectious diseases. *Climate change and human health: risks and responses*, 6, 103–137.
- Paz, S., Tourre, Y. M., & Brolley, J. (2008). Multitemporal climate variability over the Atlantic Ocean and Eurasia: linkages with Mediterranean and West African climate. *Atmospheric Science Letters*, 9(4), 196–201.
- Rogers, D. J., & Randolph, S. E. (2000). The global spread of malaria in a future, warmer world. *Science*, 289(5485), 1763–1766.
- Roudier, P., Sultan, B., Quirion, P., & Berg, A. (2011). The impact of future climate change on West African crop yields: what does the recent literature say? *Global Environmental Change*, 21(3), 1073–1083.
- Tanser, F. C., Sharp, B., & Le Sueur, D. (2003). Potential effect of climate change on malaria transmission in Africa. *The Lancet*, 362(9398), 1792–1798.
- Taylor, K. E., Stouffer, R. J., & Meehl, G. A. (2012). An overview of CMIP5 and the experiment design. *Bulletin of the American Meteorological Society*, 93(4), 485–498.
- Taylor, D., Kienberger, S., Malone, J. B., & Tompkins, A. M. (2016). Health, environmental change and adaptive capacity: mapping, examining and anticipating future risks of water-related vector-borne diseases in eastern Africa. *Geospatial Health*, 11(1 Suppl), 464.
- Tourre, Y. M., Vignolles, C., Viel, C., & Mounier, F. (2017). Climate impacts on Malaria in Northern Burkina Faso. *Geospatial Health*, 12(2). <https://doi.org/10.4081/gh.2017.600>.
- U N O O S A (2 0 1 8) <http://www.unoosa.org/oosa/en/ourwork/psa/globalhealth/activities.html>. Accessed March 2019
- Vignolles, C., Sauerbom, R., Dambach, P., Viel, C., Soubeyro, J. M., Sié, A. & Tourre, Y. M. (2016). Re-emerging Malaria vectors in rural Sahel (Nouna, Burkina Faso): the Paluclim project. *ISPRS-International Archives of the Photogrammetry, Re 276 mote Sensing and Spatial Information Sciences*, 237–242.
- Walz, Y., Wegmann, M. Dech, Raso, G. S. & Utzinger, J. (2015). *Risk profiling of schistosomiasis using remote sensing: approaches, challenges and outlook*. Parasites and Vectors, 8 (1), pp. 1–16. Springer edit. <https://doi.org/10.1186/s13071-015-0732-6> ISSN 1756–3305.
- WHO (2003). A.J., et al., (eds). *A Climate Change and Human Health: Risks and Responses* (pp. 103–132). A.J. McMichael et al., (edits). WHO, Geneva. <http://www.who.int/globalchange/publications/climchange.pdf>. Accessed March 2019
- WHO (2008). <https://www.who.net/malaria/publicatins/country-profiles/2008/mal2008-burkinafaso-en-pdf?ua=1>. Accessed March 2019
- Zhang, R., & Delworth, T. L. (2006). Impact of Atlantic multidecadal oscillations on India/Sahel rainfall and Atlantic hurricanes. *Geophysical Research Letters*, 33(17).